Spectrochimica Acta Part A: Molecular and Biomolecular Spectroscopy 260 (2021) 119953

Contents lists available at ScienceDirect

Spectrochimica Acta Part A: Molecular and Biomolecular Spectroscopy

journal homepage: www.elsevier.com/locate/saa

Novel ratiometric fluorescent probe for real-time detection of alkaline phosphatase and its application in living cells

Xiaoqian Huang [1], Xiangzhu Chen [1], Shijun Chen, Xueyan Zhang, Lin Wang, Shicong Hou *, Xiaodong Ma *

College of Science, China Agricultural University, Beijing 100193, PR China

HIGHLIGHTS

- A novel ratiometric probe was constructed to detect alkaline phosphatase.
- The introduction of spontaneously degradable linker is conducive to the construction of ratio fluorescent probes.
- The detection limit is as low as 0.16 U/L with high selectivity and accuracy;
- This probe possessing excellent biocompatibility.

GRAPHICAL ABSTRACT

Novel ratiometric fluorescent probe for real-time detection of alkaline phosphatase and its application in living cells.

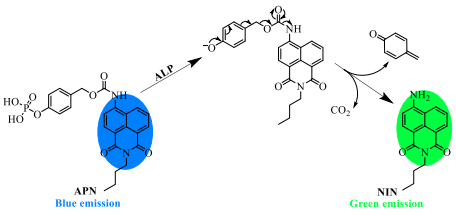

ARTICLE INFO

Article history:
Received 5 April 2021
Received in revised form 30 April 2021
Accepted 9 May 2021
Available online 12 May 2021

Keywords:
Fluorescent probe
Alkaline phosphatase
Ratiometric
Cell imaging

ABSTRACT

A novel ratiometric fluorescent probe has been developed through a simple synthetic route for the detection of alkaline phosphatase(ALP) in aqueous media and for fluorescence imaging in living cells. The introduction of a spontaneous-degradation spacer in the design of the fluorescent probe is beneficial for the ratio detection method and allows the selection of a fluorophore with an amino group. Under catalysis by ALP, the phosphate monoester bond breaks; this is followed by 1,4-elimination, decomposition of the carbamate moiety, and subsequent formation of the 4-amine-1,8-naphthalimide fluorophore. The probe ***APN*** shows a significant fluorescence colour change from blue to green in response to ALP, and the fluorescence intensity ratio of the probe solution (F_{550}/F_{480}) has a good linear relationship with the ALP concentration in the range of 0 to 100 U L^{-1}. Our studies have demonstrated that ***APN*** exhibits high accuracy in recognising ALP, with a detection limit as low as 0.16 U L^{-1}. Furthermore, the probe shows very good biocompatibility, which is beneficial for its application in biological systems.

1. Introduction

Alkaline phosphatase (ALP, EC 3.1.3.1) is a biological hydrolase that catalyses the dephosphorylation and transphosphorylation of proteins, nucleic acids, and some small biomolecules [1,2]. The enzyme plays a vital physiological role in organisms and is commonly found in bacteria, fungi, plants, and animals [3]. ALP is involved in almost every type of biological process, including metabolism, signal transduction, molecular transport, and expression of genetic information [4,5]. It is widely used as a tool enzyme in nucleic acid editing [6]. The level of ALP is an important indicator in routine blood tests. Abnormal increases in alkaline phosphatase activity in serum are associated with many diseases, including bone diseases (osteogenic bone cancer, Paget's bone disease, osteomalacia), liver diseases (cancer, hepatitis, obstructive jaundice), breast cancer, prostate cancer, and diabetes [3,7–11]. However, the level of ALP may also be reduced by metabolic disorders, such as Wilson's disease or blood system diseases, such as aplastic anaemia and chronic myeloid leukaemia [12]. Although ALP has been extensively studied, its various physiological and

* Corresponding authors.
E-mail addresses: houshc@cau.edu.cn (S. Hou), dongxm@cau.edu.cn (X. Ma).
[1] These authors contributed equally.

https://doi.org/10.1016/j.saa.2021.119953
1386-1425/

pathological functions have not been completely elucidated. In addition, the detailed mechanism of ALP activity regulation during pathogenesis remains unresolved. Therefore, accurate and sensitive detection methods need to be established to track the activity of ALP in living systems in real time.

To date, several classical colorimetric methods for the visual detection of ALP have been developed based on the biological functions of the enzyme. Substrates such as diphenyl phosphate and *p*-nitrophenyl phosphate (pNPP) were used in these methods; the compounds were dephosphorylated by ALP, producing significant colour changes, which provided a measurable relationship between the colorimetric signals and ALP activity [13,14]. These methods are characterised by short reaction times and automated procedures; they are sufficient for traditional or classic clinical trials to simply indicate advanced disease. However, to further investigate the mechanism of action of ALP in cells and even organisms and to meet the requirements for higher accuracy and sensitivity at the single-cell level, new idealised detection strategies need to be developed. Relative to traditional colorimetric methods, fluorescence analysis methods generally have the characteristics of high sensitivity, low sample volumes, strong anti-interference ability, and applicability for in situ detection and imaging [15–16].

Recently, fluorescent turn-on probes for monitoring ALP activity have been developed [17–31]. However, the single-wavelength response pattern limits the use of these probes. Unlike turn-on probes, ratiometric probes provide quantitative detection from calculations of the ratio of the emission intensities at two different wavelengths, resulting in an internal calibration effect, which improves the sensitivity and accuracy of detection [32–36]. To date, only a few ratiometric fluorescent probes for detecting ALP have been reported [37–40]. These have been constructed by direct attachment of a phosphate molecule to a hydroxy-containing fluorophore, which limits the choice of fluorophore. In addition, these probes have some limitations, such as long reaction times, requirement for organic solvents, and background fluorescence interference, which seriously affect further applications of the probes in living cells and organisms. We expected to solve these problems by designing a novel ALP ratiometric fluorescent probe.

In this study, we present a ratiometric probe for ALP (***APN***, Scheme 1) and its application to quantitative analysis of ALP activity. This probe comprises 4-amine-1,8-naphthalimide (***NIN***) as the fluorophore and phosphate-derived benzyl carbamate as the ALP hydrolytic site. We anticipated that the phosphate monoester bond of the probe would be hydrolysed by ALP; this would be followed by a series of spontaneous chemical degradation steps, and the ***NIN*** fluorophore would be released, with a redshift of the emission wavelength, allowing ratiometric fluorescence detection of ALP.

2. Materials and methods

2.1. Materials and instruments

The reagents used in the experiments were purchased from commercial sources and were of analytical grade. ALP was purchased from Sigma–Aldrich. UV/Vis absorption spectra were recorded with a PerkinElmer Lambda 650S UV/Vis spectrometer. Fluorescence spectra were recorded with a PerkinElmer LS55 fluorescence spectrometer. ^{1}H NMR and ^{13}C NMR spectra were acquired with a Bruker Avance AVII 300 MHz spectrometer. High-resolution mass spectra were acquired with an Agilent ESI-Q-TOF mass spectrometer. Live-cell imaging was performed using an Olympus IX73 inverted fluorescence microscope.

2.2. Synthesis of the probe APN

2.2.1. Synthesis of compound D2

p-Hydroxybenzaldehyde (2.5 g, 20 mmol) was dissolved in CH_3-CN (100 mL) cooled to 0 °C in an ice bath. Under stirring, diethyl chlorophosphate (4.24 g, 22 mmol) and triethylamine (0.15 mL) were added. The reaction mixture was stirred at room temperature overnight. After completion of the reaction, the solvent was evaporated to give a pale-yellow oil. The crude product was used directly for the next step without purification. The oil was dissolved in $CHCl_3$/*i*-PrOH (3:1; 300 mL) and cooled to 0 °C in an ice bath. After silica gel (10 g) was added to the reaction mixture, sodium borohydride (1.6 g, 40 mmol) was added in portions, and the mixture was allowed to react for 0.5 h. After filtration, the silica gel was washed with an appropriate amount of CH_2Cl_2. The organic phase was washed with 10% (w/w) $NaHCO_3$ solution and water, collected, and dried over anhydrous Na_2SO_4. The solvent was evaporated to dryness, and the residue was purified by column chromatography to obtain ***D2*** as a white solid in a yield of 72%. ^{1}H NMR (300 MHz, $CDCl_3$): δ = 7.32 (d, J = 8.7 Hz, 2H), 7.18 (d, J = 7.8 Hz, 2H), 4.64 (d, J = 5.7 Hz, 2H), 4.30 – 4.11 (m, 4H), 2.45 (t, J = 5.9 Hz, 1H), 1.35 ppm (td, J = 7.1, 1.0 Hz, 6H); ^{13}C NMR (75 MHz, $CDCl_3$): δ = 149.7, 137.6, 127.9, 119.6, 64.3, 64.1, 15.7 ppm.

2.2.2. Synthesis of compound EAPN

NIN-Cl was first synthesised by following the method reported previously [39]. ***NIN-Cl*** (1 mmol) was dissolved in dry CH_2Cl_2 (20 mL). ***D2*** (319 mg, 1.2 mmol) dissolved in CH_2Cl_2 (5 mL) was added dropwise to the reaction mixture at 0 °C, and the mixture was stirred at room temperature for 5 h. After the solvent was removed by rotary distillation, the residue was purified by column chromatography to obtain ***EAPN*** as a yellow solid in a yield of 95%. ^{1}H NMR (300 MHz, $CDCl_3$): δ = 8.60 – 8.48 (m, 2H), 8.39 – 8.18 (m, 3H), 7.66 (dd, J = 8.5, 7.4 Hz, 1H), 7.34 (d, J = 8.5 Hz, 2H), 7.23 – 7.10 (m, 2H), 5.21 (s, 2H), 4.28 – 4.08 (m, 6H), 1.69 (dq, J = 15.1, 7.5 Hz, 2H), 1.47 – 1.29 (m, 8H), 0.95 ppm (t, J = 7.3 Hz, 3H); ^{13}C NMR (75 MHz, $CDCl_3$): δ = 163.8, 163.3, 153.0, 150.4, 139.0, 131.9, 130.8, 129.6, 128.5, 126.5, 125.9, 122.9, 119.7, 117.5, 117.0, 66.5, 64.3, 39.8, 29.8, 20.0, 15.7, 13.4 ppm; HRMS calcd for $C_{28}H_{31}N_2O_8P$: [M + H$^+$]: 555.1891; found: 555.1885.

2.2.3. Synthesis of compound APN

Under an Ar_2 atmosphere, ***EAPN*** (110 mg, 0.198 mmol) was dissolved in dry CH_2Cl_2 (10 mL) and the mixture was cooled to 0 °C in an ice bath. TMS-Br (0.27 mL, 1.98 mmol) was added dropwise with a syringe to the reaction mixture. The ice bath was removed, and the reaction was stirred at room temperature for 48 h. After completion of the reaction, the precipitate was collected by filtration and washed with ice-cold ethyl ether. The crude product was then recrystallised from CH_3OH and ethyl acetate to afford the target product as a yellow solid in a yield of 26%. ^{1}H NMR (300 MHz, D_6-DMSO): δ = 10.32 (s, 1H), 8.67 (d, J = 8.6 Hz, 1H), 8.44 (t, J = 7.8 Hz, 2H), 8.18 (d, J = 8.3 Hz, 1H), 7.78 (dd, J = 8.5, 7.4 Hz, 1H), 7.48 (d, J = 8.5 Hz, 2H), 7.20 (d, J = 8.2 Hz, 2H), 5.22 (s, 2H), 4.07 – 3.94 (m, 2H), 1.69 – 1.45 (m, 2H), 1.33 (dq, J = 14.4, 7.3 Hz, 2H), 0.90 ppm (t, J = 7.3 Hz, 3H); ^{13}C NMR (75 MHz, DMSO): δ = 163.5, 163.0, 154.0, 151.7, 140.8, 131.7 (d, J = 2.8 Hz), 130.9, 129.9, 129.3, 128.4, 126.4, 123.9, 122.3, 120.2, 118.1, 117.1, 66.3, 39.4, 29.8, 19.9, 13.8 ppm (s); HRMS calcd for $C_{24}H_{23}N_2O_8P$: [M + H$^+$] 499.1265; found: 499.1263.

2.3. APN and NIN solution for fluorescence detection

APN and ***NIN*** were dissolved in dimethyl sulfoxide (DMSO) as a sample stock solution (2 mM). Tris-HCl (10 mM, pH 8) buffer solu-

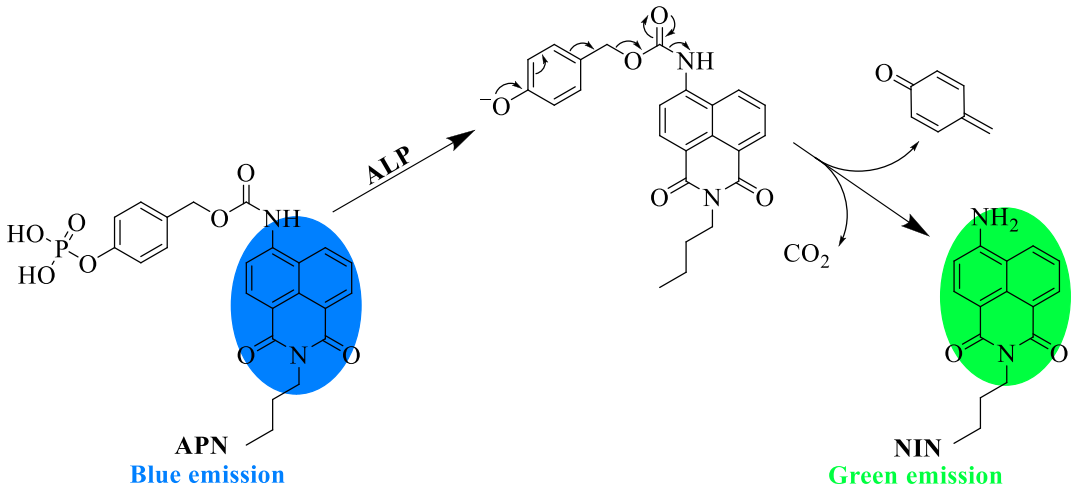

Scheme 1. Structure of ***APN*** and mechanism for detecting ALP.

tion was used as the solvent in spectroscopy experiments unless otherwise stated. In the UV–vis spectrum and fluorescence spectrometry experiments, 5 μL of ***APN*** and 5 μL of ***NIN*** were dissolved in 2 mL of buffer solution for measurement, and the final measured concentration was 5 μM. Because the enzyme requires a milder and more stable environment in the organism, in order to better detect the activity of ALP, all experiments were carried out at 37 °C.

2.4. Cell culture

Live MDBK cells (Madin-Darby bovine kidney cells) and HeLa cells (cervical cancer cells) were provided by the College of Veterinary Medicine, China Agricultural University (Beijing,China). All cells were cultured in Dulbecco's modified Eagle's medium (DMEM) containing 10% fetal bovine serum and 1% penicillin/streptomycin under ambient conditions of 5% CO_2 at 37 °C.

2.5. Cytotoxicity assay

The cytotoxicity of ***APN*** in cells was determined using a standard 5-dimethylthiazol-2-yl-2,5-diphenyltetrazolium bromide (MTT) assay. The cells were seeded into a 96-well plate in the presence of 100 μL of DMEM and allowed to adhere for 24 h. The cells were then incubated with different concentrations of ***APN*** (0, 5, 10, 20, 40,80 mM, containing 0.5% DMSO) for 24 h. After the medium was removed, 100 μL of MTT (5 mg/mL) solution was added to each well, and the cells were further cultured under the same conditions for 4 h. After removing the MTT solution, 100 μL of DMSO was added, and the absorbance of each well was read at 570 nm. Cell viability was calculated by assuming 100% cell viability for the control cells without ***APN*** treatment.

2.6. Living cell imaging

HeLa cells were cultured in DMEM (without FBS) for 30 min with the addition of ***APN*** (5 μM). Another group of HeLa cells was first treated with the Na_3VO_4 as a typical inhibitor of ALP, cultured for 30 min, and then further cultured for 30 min with ***APN*** (5 μM).The residual ***APN*** was washed away and the cells were subjected to imaging experiments.

3. Results and discussion

3.1. Synthesis and characterization

The detailed synthesis steps for ***APN*** are illustrated in Scheme 2 and described in the Materials and Methods section. Diethyl chlorophosphate was treated with *p*-hydroxybenzaldehyde to form compound ***D1***, which was subsequently reduced with $NaBH_4$ to form compound ***D2***. Previously prepared ***NIN-Cl*** was connected to compound ***D2***, and the product was subsequently deprotected to give the target compound ***APN***. The structure of the compound ***APN*** was confirmed by ^{1}H NMR, ^{13}C NMR, and HRMS (see Electronic Supplementary Material (ESM) Fig. S6–8*).

3.2. Fluorescence properties of the probe to ALP

The photophysical properties of the ***APN*** probe and the ***NIN*** fluorophore were first determined. ***APN*** and ***NIN*** exhibit absorption maxima (λ_{abs}) at 370 nm and 430 nm, respectively, with corresponding emission maxima (λ_{fl}) at 480 nm (Φ = 0.19) and 550 nm (Φ = 0.28) (see ESM Fig. S1* and Table S1*). The higher fluorescence quantum yield of the fluorophore allows it to have higher fluorescence brightness, and the larger Stokes shift effectively prevents self-absorption of fluorescence.

The reaction of the probe with ALP to generate the fluorophore was confirmed by HPLC, with the results corresponding to the disappearance of ***APN*** (t_R = 3.2 min) and the presence of ***NIN*** (t_R = 6.5-min) (ESM Fig. S2*); this verifies the anticipated mechanism (Scheme 1). The emission spectra of a 5 μM solution of ***APN*** treated with ALP in Tris-HCl buffer (10 mM, pH 8.0, 37 °C) show a gradual increase at 550 nm with a concomitant decrease at 480 nm (Fig. 1a). As the concentration of ALP increases, the activity of the enzyme-catalysed reaction increases, so the time required for the fluorescence emission intensity ratio (F_{550}/F_{480}) to stabilise tends to be shorter (Fig. 1b). With 400 U L^{-1} of ALP in the solution of ***APN***, the F_{550}/F_{480} ratio tends to be stable after approximately 12 min, and this response rate is faster than most of the reported ALP probes. The Michaelis–Menten constant (K_m) of the ALP-catalysed reaction was determined to be 2.78 μM; this low K_m value indicates that ALP has a high affinity for the probe (ESM Fig. S3*).

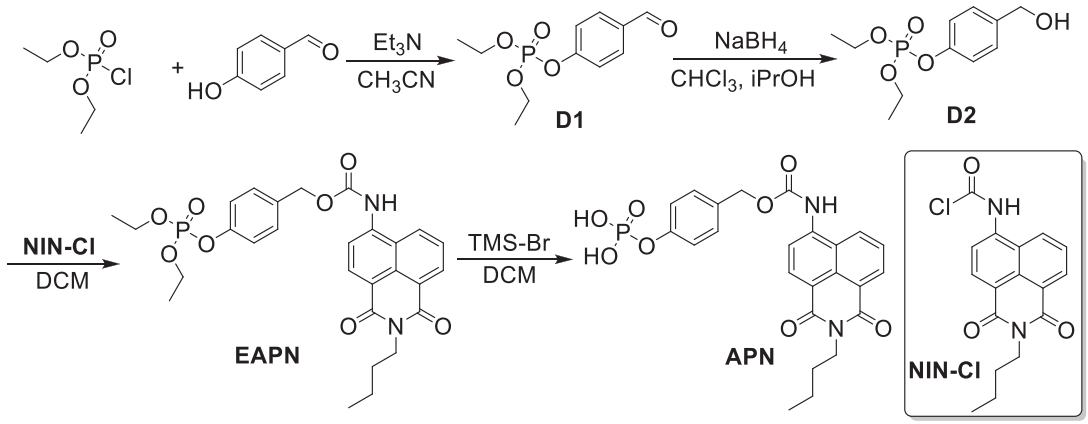

Scheme 2. Synthetic route to ***APN***.

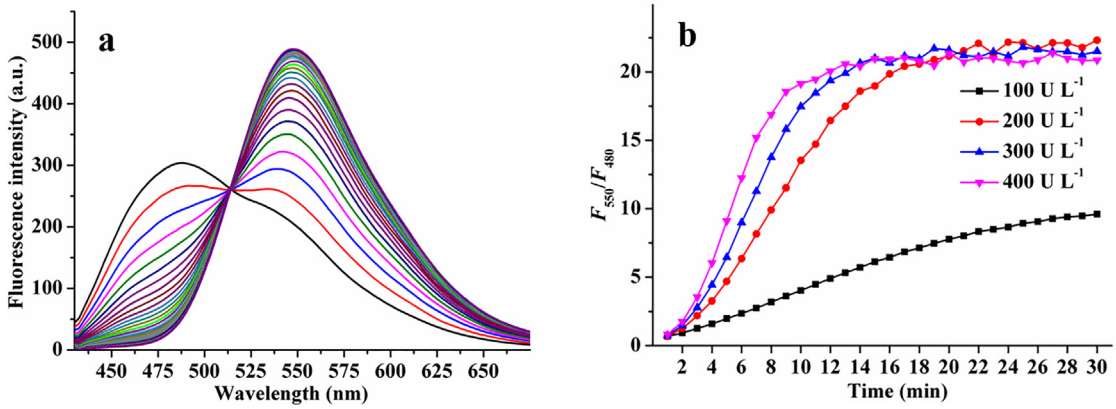

Fig. 1. (a) Fluorescence spectra changes of a solution of ***APN*** varied with time in the presence of 100 U L^{-1} of ALP. Conditions: Tris-HCl buffer (10 mM, pH 8.0, 0.25% DMSO), 37 °C, λ_{ex} = 415 nm. (b) F_{550}/F_{480} ratios of the fluorescence intensity of solutions of ***APN*** over time in the presence of different concentrations of ALP.

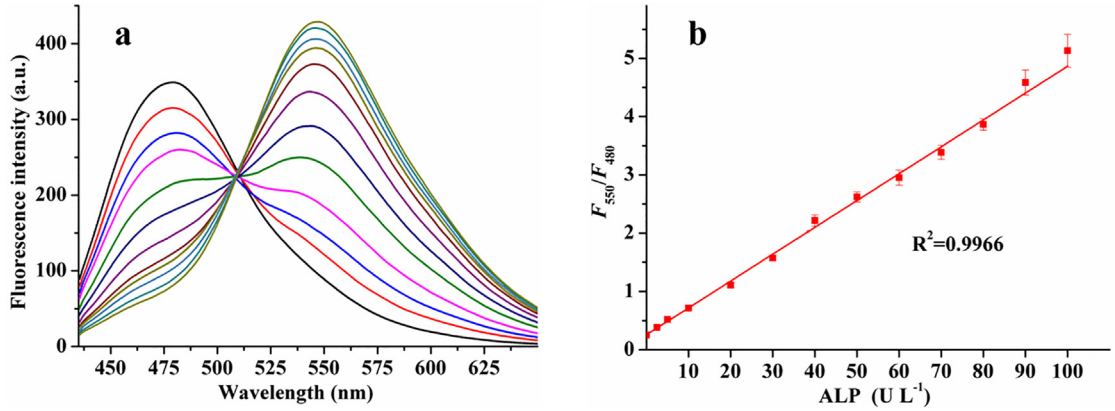

Fig. 2. (a) Fluorescence spectra changes of a solution of ***APN*** in the presence of different concentrations of ALP. (b) Plot of the F_{550}/F_{480} ratios for ***APN*** versus the concentration of ALP. Data were obtained 10 min after ALP addition at 37 °C in Tris-HCl buffer (10 mM, pH 8.0, 0.25% DMSO), λ_{ex} = 415 nm.

Under consistent conditions (reaction at 37 °C for 10 min in Tris-HCl buffer (10 mM, pH 8.0, 0.25% DMSO)), enzyme activity was quantitatively detected from the F_{550}/F_{480} ratio change of a solution of ***APN***. A plot of F_{550}/F_{480} ratios against ALP concentrations ranging from 0 to 100 U L^{-1} shows a linear relationship (R^2 = 0.9966), and the detection limit was calculated to be 0.16 U L^{-1} (Fig. 2). Furthermore, the probe is insensitive to pH values ranging from 3 to 10 (ESM Fig. S4*). These results demonstrate that the probe can be used to sensitively detect ALP levels in biological systems.

The selectivity and anti-interference of ***APN*** for a variety of common biological enzyme species, biomolecules, and ions was examined. Only slight fluctuations in the F_{550}/F_{480} fluorescence ratio occur upon the addition of cellulase (Cel), lysozyme (Lyso), β-galactosidase (β-Gal), β-glucuronidase (β-Glu), bovine serum albumin (BSA), ovalbumin (OVA), human serum albumin (HSA), cysteine (Cys), homocysteine (Hcy), glutathione (GSH), vitamin C (Vc), hydrogen peroxide (H_2O_2), hydrogen sulfide (H_2S), $CaCl_2$, $MgCl_2$, and foetal bovine serum (FBS) (Fig. 3). However, as the ALP continues to be added to the above system in the presence

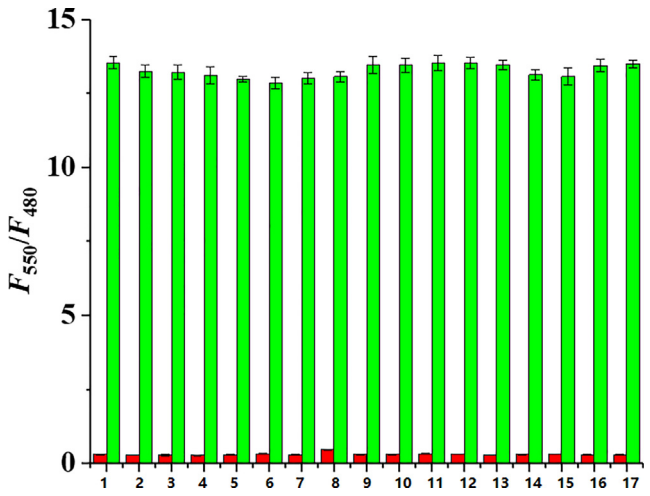

Fig. 3. Selective and anti-interference experiments of the probe for various biological enzyme species, biomolecules, and ions. Tris-HCl buffer (10 mM, pH 8.0, 0.25% DMSO) was used as the reaction system. Various analytes were added to the probe solution and then allowed to react at 37 °C for 10 min. λex = 415 nm. ***APN*** upon addition of different species (red bars), and fluorescence changes of the mixture of ***APN*** and ALP after addition of an excess of the Interference species (green bars).The concentrations of the various analytes were as follows: 1.ALP (200 U L^{-1}), 2.Cel (1 U mL^{-1}), 3.Lyso (1 U mL^{-1}), 4.β-Gal (1 U mL^{-1}), 5.β-Glu (1 U mL^{-1}), 6. BSA (100 μg mL^{-1}), 7.OVA (100 μg mL^{-1}), 8.HSA (100 μg mL^{-1}), 9.Cys (100 μM), 10. Hcy (100 μM), 11.GSH (100 μM), 12.Vc (100 μM), 13·H_2O_2 (100 μM), 14.H_2S (100 μM), 15.$CaCl_2$ (100 μM), 16.$MgCl_2$ (100 μM), 17.FBS (100 μg mL^{-1}).

of ALP, the fluorescence ratio is significantly increased (Fig. 3); this is accompanied by a distinct redshift of the fluorescence wavelength (Fig. 2a), which corresponds to the evolution of the ***NIN*** fluorophore. These results indicate that ***APN*** has excellent selectivity and interference resistance toward ALP over other competitive analytes, which meets the need for accurate detection in actual samples.

3.3. Fluorescence imaging in living cells

Furthermore, the applicability of ***APN*** for imaging ALP activity in live cells was investigated. First, the toxicity of the probe to MDBK cells was investigated with an MTT assay. The probe shows low cytotoxicity in vitro (ESM Fig. S5*); this will facilitate the use of the probe for fluorescence imaging of ALP in living cells. HeLa cells that can overexpress endogenous ALP[41–42] were used in cell imaging experiments. When HeLa cells were treated with ***APN***, a strong signal was observed in the green channel, whereas there was an extremely weak signal in the blue channel (Fig. 4). For comparison, HeLa cells were pretreated with an inhibitor (Na_3VO_4) before treatment with the probe; in this case, dim fluorescence was observed in the green channel, whereas very bright fluorescence occurred in the blue channel. These results reveal that ***APN*** is applicable to the detection and imaging of overexpression of endogenous ALP in HeLa cells.

4. Conclusion

In summary, a new ratiometric fluorescence assay for ALP activity was established using the novel ***APN*** probe. The use of a self-immolative spacer increased the variety of potential fluorophores and allowed the selection of amine-containing fluorophores. The probe showed a marked blue-to-green change in the emitted colour in response to ALP. Most importantly, the probe showed a rapid, accuracy, and selective fluorescence sensing effect for ALP in Tris-HCl buffer, with a detection limit as low as 0.16 U L^{-1}. This probe possesses excellent biocompatibility and can be used to visualise endogenous ALP in cervical cancer cells.

Funding information

This work was supported by the National Key Technology Research and Development Program (No. 2015BAK45B01).

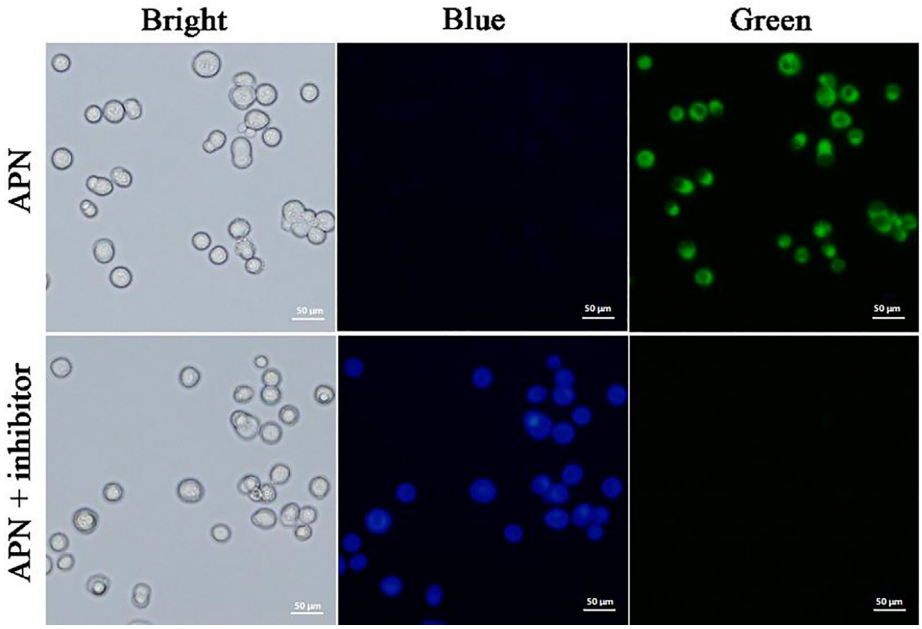

Fig. 4. (a) Fluorescence images of HeLa cells incubated with ***APN*** for 30 min. (b) Fluorescence images of HeLa cells pretreated with 1 mM Na_3VO_4 for 30 min and then treated with ***APN*** for 30 min.

CRediT authorship contribution statement

Xiaoqian Huang: Conceptualization, Methodology, Software, Writing - original draft, Writing - review & editing, Validation. **Xiangzhu Chen:** Conceptualization, Methodology, Software, Writing - original draft, Writing - review & editing, Validation. **Shijun Chen:** Investigation, Formal analysis, Software. **Xueyan Zhang:** Investigation, Software. **Lin Wang:** Software. **Shicong Hou:** Supervision, Project administration, Funding acquisition. **Xiaodong Ma:** Supervision.

Declaration of Competing Interest

The authors declare that they have no known competing financial interests or personal relationships that could have appeared to influence the work reported in this paper.

Appendix A. Supplementary material

Supplementary data to this article can be found online at https://doi.org/10.1016/j.saa.2021.119953.

References

[1] J.E. Coleman, Structure and mechanism of alkaline phosphatase, Annu. Rev. Biophys. Biomol. Struct. 21 (1) (1992) 441–483, https://doi.org/10.1146/annurev.bb.21.060192.002301.

[2] N.K. Tonks, Protein tyrosine phosphatases: from genes, to function, to disease, Nat. Rev. Mol. Cell Bio. 7 (11) (2006) 833–846, https://doi.org/10.1038/nrm2039.

[3] J.L. Millan, Alkaline phosphatases: Structure, substrate specificity and functional relatedness to other members of a large superfamily of enzymes, Purinerg. Signal 2 (2) (2006) 335–341, https://doi.org/10.1007/s11302-005-5435-6.

[4] Y.S. Torisawa, N. Ohara, K. Nagamine, et al., Electrochemical Monitoring of Cellular Signal Transduction with a Secreted Alkaline Phosphatase Reporter System, Anal. Chem. (Washington DC U S). 78 (22) (2006) 7625–7631, https://doi.org/10.1021/ac060737s.

[5] A.C. Hahnel, D.A. Rappolee, J.L. Millan, et al., Two alkaline phosphatase genes are expressed during early development in the mouse embryo, Development (Cambridge, U.K.) 110 (2) (1990) 555–564, PMID:2133555.

[6] A.M. Maxam, W. Gilbert, Sequencing end-labeled DNA with base-specific chemical cleavages, Method Enzymol. 65 (1) (1980) 499–560, https://doi.org/10.1016/S0076-6879(80)65059-9.

[7] V.O. Van Hoof, M.E. De Broe, Interpretation and clinical significance of alkaline phosphatase isoenzyme patterns, Crit. Rev. Cl Lab. Sci. 31 (3) (1994) 197–293, https://doi.org/10.3109/10408369409084677.

[8] C.H.S. Lu, K. Liu, L.P. Tan, et al., Current Chemical Biology Tools for Studying Protein Phosphorylation and Dephosphorylation, Chem-Eur. J. 18 (1) (2012) 28–39, https://doi.org/10.1002/chem.201103206.

[9] P.L. Wolf, Clinical significance of serum high-molecular-mass alkaline phosphatase, alkaline phosphatase-lipoprotein-X complex, and intestinal variant alkaline phosphatase, J. Clin. Lab. Anal. 8 (3) (2010) 172–176, https://doi.org/10.1002/jcla.1860080311.

[10] K. Ooi, K. Shiraki, Y. Morishita, et al., High-molecular intestinal alkaline phosphatase in chronic liver diseases, J. Clin. Lab. Anal. 21 (3) (2010) 133–139, https://doi.org/10.1002/jcla.20178.

[11] B.A. Rader, Alkaline phosphatase, an unconventional immune protein 897/1-897/6 Front. Immunol. 8 (2017), https://doi.org/10.3389/fimmu.2017.00897.

[12] E.G. Giannini, R. Testa, V. Savarino, Liver enzyme alteration: a guide for clinicians, Can. Med. Assoc. J. 172 (3) (2005) 367–379, https://doi.org/10.1503/cmaj.1040752.

[13] O.A. Bessey, O.H. Lowry, M.J. Brock, Method for the determination of alkaline phosphatase with five cubic millimeters of serum, J. Biol. Chem. 164 (1946) 321–329, https://doi.org/10.1016/j.iccn.2014.08.002.

[14] R. Breslow, I. Katz, Relative reactivities of p-nitrophenyl phosphate and phosphorothioate toward alkaline phosphatase and in aqueous hydrolysis, J. Am. Chem. Soc. 90 (26) (1968) 7376–7377, https://doi.org/10.1021/ja01028a054.

[15] Y.L. Yue, A.B. Yan, H.W. Rui, et al., FRET-based ratiometric fluorescent detection of arginine in mitochondrion with a hybrid nanoprobe, Chin. Chem. Lett. 31 (2) (2020) 443–446, https://doi.org/10.1016/j.cclet.2019.07.047.

[16] Z. Li, W. Zhang, C. Liu, et al., A colorimetric and ratiometric fluorescent probe for hydrazine and its application in living cells with low dark toxicity[J]. Sensors & Actuators B, Chemical 241(mar.):665–671 (2017), https://doi.org/10.1016/j.snb.2016.10.141.

[17] L. Xu, X. He, Y. Huang, et al., A novel near-infrared fluorescent probe for detecting intracellular alkaline phosphatase and imaging of living cells, J Mater Chem B. (2019), https://doi.org/10.1039/C8TB03230K, Ahead of Print.

[18] W. Zhang, H. Yang, N. Li, et al., A sensitive fluorescent probe for alkaline phosphatase and an activity assay based on the aggregation-induced emission effect, RSC Adv. 8 (27) (2018) 14995–15000, https://doi.org/10.1039/C8RA01786G.

[19] L. Xu, X. He, P. Ma, et al., A water-soluble fluorescent probe for the sensitive detection of endogenous alkaline phosphatase in living cells, Dyes Pigments. 159 (2018) 584–589, https://doi.org/10.1016/j.dyepig.2018.07.023.

[20] M. Lin, J. Huang, F. Zeng, et al., A Fluorescent Probe with Aggregation-Induced Emission for Detecting Alkaline Phosphatase and Cell Imaging, Chem-Asian J. (2018), https://doi.org/10.1002/asia.201801540, Ahead of Print.

[21] Z. Gao, J. Sun, M. Gao, et al., A unique off-on near-infrared cyanine-based probe for imaging of endogenous alkaline phosphatase activity in cells and in vivo, Sensor Actuat B-chem. 265 (2018) 565–574, https://doi.org/10.1016/j.snb.2018.03.078.

[22] Y. Tan, L. Zhang, K.H. Man, et al., Reaction-Based Off-On Near-infrared Fluorescent Probe for Imaging Alkaline Phosphatase Activity in Living Cells and Mice, Acs Appl Mater Inter. 9 (8) (2017) 6796–6803, https://doi.org/10.1021/acsami.6b14176.

[23] H.W. Liu, X.X. Hu, L. Zhu, et al., In vivo imaging of alkaline phosphatase in tumor-bearing mouse model by a promising near-infrared fluorescent probe, Talanta 175 (2017) 421–426, https://doi.org/10.1016/j.talanta.2017.04.081.

[24] S.J. Li, C.Y. Li, Y.F. Li, et al., Facile and Sensitive Near-Infrared Fluorescence Probe for the Detection of Endogenous Alkaline Phosphatase Activity In Vivo, Anal Chem (Washington DC U S). 89 (12) (2017) 6854–6860, https://doi.org/10.1021/acs.analchem.7b01351.

[25] H.M. Zhang, C.L. Xu, J. Liu, et al., An enzyme-activatable probe with a self-immolative linker for rapid and sensitive alkaline phosphatase detection and cell imaging through a cascade reaction, Chem. Commun (Cambridge U K). 51 (32) (2015) 7031–7034, https://doi.org/10.1039/C5CC01005E.

[26] H.T. Zhang, P. Xiao, Y.T. Wong, et al., Construction of an alkaline phosphatase-specific two-photon probe and its imaging application in living cells and tissues, Biomaterials 140 (2017) 220–229, https://doi.org/10.1016/j.biomaterials.2017.06.032.

[27] Q. Hu, F. Zeng, C. Yu, et al., A fluorescent probe for alkaline phosphatase via excited state intramolecular proton transfer, Sensor Actuat. B-chem. 220 (2015) 720–726, https://doi.org/10.1016/j.snb.2015.05.111.

[28] X. Gu, G. Zhang, Z. Wang, et al., A new fluorometric turn-on assay for alkaline phosphatase and inhibitor screening based on aggregation and deaggregation of tetraphenylethylene molecules, Analyst (Cambridge U K). 138 (8) (2013) 2427–2431, https://doi.org/10.1039/c3an36784c.

[29] T.I. Kim, H. Kim, Y. Choi, et al., A fluorescent turn-on probe for the detection of alkaline phosphatase activity in living cells, Chem. Commun. (Cambridge U K). 47 (35) (2011) 9825–9827, https://doi.org/10.1039/c1cc13819g.

[30] M. Kawaguchi, K. Hanaoka, T. Komatsu, et al., Development of a highly selective fluorescence probe for alkaline phosphatase, Bioorg. Med. Chem. Lett. 21 (17) (2011) 5088–5091, https://doi.org/10.1016/j.bmcl.2011.03.070.

[31] X. Zhu, Q. Liu, C. Jiang, 8-Quinolyl phosphate as a substrate for the fluorometric determination of alkaline phosphatase, Clin. Chim. Acta 377 (1–2) (2007) 150–153, https://doi.org/10.1016/j.aca.2006.03.067.

[32] B. Ma, F. Zeng, X. Li, et al., A facile approach for sensitive, reversible and ratiometric detection of biothiols based on thymine-mediated excimer-monomer transformation, Chem Commun (Cambridge U K). 48 (48) (2012) 6007–6009, https://doi.org/10.1039/c2cc32064a.

[33] C. Yu, X. Li, F. Zeng, et al., Carbon-dot-based ratiometric fluorescent sensor for detecting hydrogen sulfide in aqueous media and inside live cells, Chem Commun (Cambridge U K). 49 (4) (2013) 403–405, https://doi.org/10.1039/c2cc37329g.

[34] C. Huang, T. Jia, M. Tang, et al., Selective and Ratiometric Fluorescent Trapping and Quantification of Protein Vicinal Dithiols and in Situ Dynamic Tracing in Living Cells, J. Am. Chem. Soc. 136 (40) (2014) 14237–14244, https://doi.org/10.1021/ja5079656.

[35] X. Zhang, Y. Zhou, X. Gu, et al., Synthesis of a selective ratiometric fluorescent probe based on Naphthalimide and its application in human cytochrome P450 1A, Talanta 186 (2018) 413–420, https://doi.org/10.1016/j.talanta.2018.04.079.

[36] Z. Zhou, F. Wang, G. Yang, et al., A Ratiometric Fluorescent Probe for Monitoring Leucine Aminopeptidase in Living Cells and Zebrafish Model, Anal. Chem. (Washington DC U S). 89 (21) (2017) 11576–11582, https://doi.org/10.1021/acs.analchem.7b02910.

[37] Q. Zhang, S. Li, C. Fu, et al., Near-infrared mito-specific fluorescent probe for ratiometric detection and imaging of alkaline phosphatase activity with high sensitivity, J. Mater. Chem. B 7 (3) (2019) 443–450, https://doi.org/10.1039/C8TB02799D.

[38] X. Zhou, Y. Jiang, X. Zhao, et al., A new two-photon ratiometric fluorescent probe for detecting alkaline phosphatase in living cells, Molecules 21 (12) (2016) 1619/1–1619/10, https://doi.org/10.3390/molecules21121619.

[39] C. Fan, S. Luo, H. Qi, A ratiometric fluorescent probe for alkaline phosphatase via regulation of excited-state intramolecular proton transfer, Luminescence 31 (2) (2016) 423–427, https://doi.org/10.1002/bio.2977.

[40] X. Hou, Q. Yu, F. Zeng, et al., A ratiometric fluorescent probe for in vivo tracking of alkaline phosphatase level variation resulting from drug-induced organ damage, J. Mater. Chem. B 3 (6) (2015) 1042–1048, https://doi.org/10.1039/C4TB01744G.

[41] X. Chen, X. Ma, Y. Zhang, et al., Ratiometric fluorescent probes with a self-immolative spacer for real-time detection of β-galactosidase and imaging in living cells, Anal. Chim. Acta 1033 (2018) 193–198, https://doi.org/10.1016/j.aca.2018.05.071.

[42] F. Schmid, R. Fliegert, T. Westphal, et al., Nicotinic acid adenine dinucleotide phosphate (NAADP) degradation by alkaline phosphatase, J. Biol. Chem. 287 (39) (2012) 32525–32534, https://doi.org/10.1074/jbc.M112.362715.